

UC Irvine

UC Irvine Previously Published Works

Title

Preclinical Evaluation of Off-The-Shelf PD-L1+ Human Natural Killer Cells Secreting IL15 to Treat Non-Small Cell Lung Cancer.

Permalink

<https://escholarship.org/uc/item/0pv336dc>

Journal

Cancer Immunology Research, 12(6)

Authors

Lu, Ting

Ma, Rui

Mansour, Anthony

et al.

Publication Date

2024-06-04

DOI

10.1158/2326-6066.CIR-23-0324

Peer reviewed



Published in final edited form as:

Cancer Immunol Res. 2024 June 04; 12(6): 731–743. doi:10.1158/2326-6066.CIR-23-0324.

Preclinical Evaluation of Off-The-Shelf PD-L1⁺ Human Natural Killer Cells Secreting IL15 to Treat Non-Small Cell Lung Cancer

Ting Lu^{1,2,†}, Rui Ma^{1,†}, Anthony G. Mansour^{1,†}, Christian Bustillos^{1,†}, Zhiyao Li¹, Zhenlong Li¹, Shoubao Ma¹, Kun-Yu Teng¹, Hanyu Chen¹, Jianying Zhang³, Miguel A. Villalona-Calero^{4,5}, Michael A. Caligiuri^{1,2,5,*}, Jianhua Yu^{1,2,5,6,*}

¹Department of Hematology and Hematopoietic Cell Transplantation, City of Hope National Medical Center, Los Angeles, CA 91010, USA.

²Hematologic Malignancies Research Institute, City of Hope National Medical Center, Los Angeles, CA 91010, USA.

³Department of Computational and Quantitative Medicine, City of Hope National Medical Center, Los Angeles, CA 91010, USA.

⁴Department of Medical Oncology and Therapeutics Research, City of Hope National Medical Center, Los Angeles, CA 91010, USA.

⁵City of Hope Comprehensive Cancer Center, Los Angeles, CA 91010, USA.

⁶Department of Immuno-Oncology, Beckman Research Institute of City of Hope, Los Angeles, CA 91010, USA.

Abstract

We described previously a human natural killer (NK) cell population that upregulates PD-L1 expression upon recognizing and reacting to tumor cells or exposure to a combination of IL12, IL18 and IL15. Here, to investigate the safety and efficacy of tumor-reactive and cytokine-activated (TRACK) NK cells, human NK cells from umbilical cord blood were expanded, transduced with a retroviral vector encoding soluble (s) IL15, and further cytokine activated to induce PD-L1 expression. Our results show cryopreserved and thawed sIL15_TRACK NK cells had significantly improved cytotoxicity against non-small cell lung cancer (NSCLC) *in vitro* when compared to non-transduced (NT) NK cells, PD-L1⁺ NK cells lacking sIL15 expression (NT_TRACK NK), or NK cells expressing sIL15 without further cytokine activation (sIL15 NK cells). Intravenous injection of sIL15_TRACK NK cells into immunodeficient mice with NSCLC significantly slowed tumor growth and improved survival when compared to NT NK

*Corresponding authors. Michael A. Caligiuri, MD, mcaligiuri@coh.org and Jianhua Yu, PhD, jiayu@coh.org.

†Equally contributing authors

Author contributions:

Conceptualization: JY, MAC

Methodology or Experiments: TL, AGM, RM, CB, ZL, KT, CY, SM, ZL

Investigation: TL

Analysis and Interpretation: TL, JZ

Funding acquisition: JY, MAC

Supervision: JY, MAC

Writing, review, & editing: TL, JY, MAC

Competing interests: The remaining authors have no conflicts of interest to disclose.

and sIL15 NK cells. The addition of the anti-PD-L1 atezolizumab further improved control of NSCLC growth by sIL15_TRACK NK cells *in vivo*. Moreover, a dose-dependent efficacy was assessed for sIL15_TRACK NK cells without observed toxicity. These experiments indicate that the administration of frozen, off-the-shelf allogeneic sIL15_TRACK NK cells is safe in preclinical models of human NSCLC and has potent antitumor activity without and with the administration of atezolizumab. A Phase I clinical trial modeled after this preclinical study using sIL15_TRACK NK cells alone or with atezolizumab for relapsed or refractory NSCLC is currently underway ([NCT05334329](#)).

Keywords

NK cell; lung cancer; preclinical; PD-L1; immunotherapy

Introduction

Lung cancer is the leading cause of cancer-related mortality not only in the United States but also worldwide, with 85% of cases accounted for as non-small cell lung cancer (NSCLC) (1). Immune checkpoint blockade (ICB) of programmed death-1 (PD-1) or its ligand PD-L1 have set a new standard of care for the first-line treatment of advanced NSCLC, either as monotherapy or combined with chemotherapy (2–8). Although ICB has shown impressive tumor regression in patients with advanced NSCLC, lasting responses have been limited to 15% of eligible patients (9). This high failure rate of ICB therapy is a result, at least in part, of low tumor PD-L1 expression, along with immune suppression within the tumor microenvironment (10). Thus, the overall prognosis for advanced stage NSCLC remains poor.

Natural killer (NK) cells are innate lymphocytes with cytotoxic activity against virally infected and tumor cells mediated in part by the recognition of the target cell and the subsequent release of cytokines and cytotoxic granules (11). They can be activated against target cells without any prior exposure or priming and are not restricted by major histocompatibility (MHC) antigen expression, yet do not mediate graft-versus-host disease (GVHD) in the setting of allogeneic stem cell transplantation (12,13), thus opening the door for off-the-shelf allogeneic NK-cell therapy. In our previous study (14), we described the identification of an NK-cell population that upregulated PD-L1 upon recognizing and reacting to tumor or upon exposure to a combination of inflammatory cytokines IL12, IL15, and IL18. PD-L1⁺ NK cells are more potent against tumor cells than their PD-L1⁻ counterparts. Furthermore, the administered anti-PD-L1 atezolizumab acts directly upon PD-L1⁺ NK cells via a p38–NFκB pathway to induce the degranulation of perforin, enhance secretion of IFN-γ, and further upregulate PD-L1 expression via a positive feedback loop (14).

In the current study, we utilized human umbilical cord blood (UCB) NK cells to generate NK cells secreting soluble (s) human IL15 and cytokine-induced expression of PD-L1, which we referred to as tumor-reactive and cytokine-activated killer (TRACK) NK cells. We assessed the functional activity of cryopreserved sIL15_TRACK NK cells to recognize

and lyse NSCLC tumor cells *in vitro* and *in vivo*, compared to non-transduced (NT) NK cells, PD-L1⁺ NK cells lacking sIL15 expression (NT_TRACK NK), or NK cells expressing sIL15 without further cytokine activation (sIL15 NK cells). Furthermore, we evaluated safety, toxicity, tumor control, and survival using an immunodeficient mouse model of human NSCLC treated with sIL15_TRACK NK cells in the absence and presence of atezolizumab.

Methods and Materials

Ethics statement

All experiments and handling of mice were conducted under federal, state, and local guidelines and with approval from City of Hope's Institutional Animal Care and Use Committee. Human UCB units for both research and clinical grade work were obtained from StemCyte Inc. (Baldwin Park, CA), under protocols approved by the City of Hope Institutional Review Board. Blood cones for T-cell isolation were obtained from the Michael Amini Transfusion Medicine Center at the City of Hope National Medical Center under institutional review board-approved protocols.

Cell lines

A549 (Cat# CCL-185) and H460 (Cat # HTB-177) NSCLC cell lines were purchased from American Type Culture Collection (ATCC) in 2021 and cultured in Dulbecco's Modified Eagle Medium (DMEM) (Gibco, Cat# 11965092) supplemental with 10% fetal bovine serum (FBS) (Gibco, Cat# 16000044) and 1% GlutaMax (Gibco, Cat# 35050061). K562 feeder cells, which co-express 4-1BBL and membrane bound IL21, were gifted by CytoImmune Therapeutics, Inc and cultured in RPMI 1640 medium (Gibco, Cat# 11875093) supplemented with 10% FBS. No authentication of these cell lines was performed after they were purchased or received. Cell morphology and growth characteristics were monitored during the study to ensure their authenticity. All these cell lines were routinely tested for the absence of Mycoplasma using the MycoAlert Mycoplasma Detection Kit from Lonza (Cat# LT07-318). All cell lines used in experiments were cultured for less than 10 passages.

Plasmid construction and retrovirus production

The retroviral vectors encoding sIL15_and truncated (t) EGFR, PD-L1, or a firefly luciferase_ZsGreen (FFLuc) gene were constructed after multiple steps of PCR amplification, gel electrophoresis and extraction, enzyme digestion, ligation, transformation, and plasmid extraction. Retroviral particles were produced as previously described (15).

To generate the firefly luciferase (FFLuc)-expressing A549 (A549-Luc) cell line or H460 cell line (H460-Luc), and the PD-L1 overexpressed A549-Luc (A549^{PD-L1}-Luc) cell line, retroviral transduction with RetroNectin (Takara Bio, Cat# T100B) was performed according to the manufacturer's protocol.

NK-cell and T-cell isolation and expansion

UCB NK cells were isolated from UCB using RosetteSepTM Human NK Cell Enrichment Cocktail (STEMCELL, Cat# 15065) followed by a density-gradient centrifugation with

Ficoll-Paque PLUS (Cytiva, Cat# 17144003). Cryopreserved primary human NK cells were stimulated with irradiated (100 Gy) K562 feeder cells at effector:target (E:T) ratio of 2:1 and recombinant human IL2 (Proleukin) in complete serum-free stem cell growth medium (SCGM) (CellGenix, Cat# 20802–0500) on day 0. Activated and expanded NK cells were placed on recombinant human fibronectin-coated plates (TakaraBio, Cat# T100B) and infected with a retrovirus containing sIL15 and tEGFR following the manufacturer's instructions. On day 9, NK cells were stimulated again with irradiated K562 feeder cells in the presence of IL2. On day 16, NK cells were stimulated with IL12 (10 ng/mL) (Akron Bio, Cat# AK9995–0100) and IL18 (10 ng/mL) (Akron Bio, Cat# AK9999–0025). The efficiency of transduction was determined using flow cytometric analysis to assess tEGFR expression on day 17 when NK cells were harvested and cryopreserved in liquid nitrogen (LN2) for use in the indicated assays (see Flow cytometry). Cell count and viability were measured by using a Guava Muse Cell Analyzer (Luminex) according to the standard operating procedure (SOP). All assays performed in this study were performed with cryopreserved NK cells.

In addition to sIL15_TRACK NK cells, 3 groups of control NK cells were manufactured with modifications to the process described above: NK cells without transduction or further cytokine activation (NT NK cells), NK cells without transduction but with further cytokine activation (NT_TRACK NK cells), or NK cells with transduction but without further cytokine activation (sIL15 NK cells). Cryopreserved and thawed NK cells were used in all *in vitro* and *in vivo* experiments.

For experiments that included T cells, we isolated polyclonal T cells from blood cones provided by Michael Amini Transfusion Medicine Center immediately after blood donation from healthy people). T cells were activated *ex vivo* using CTS Dynabeads CD3/CD28 (Gibco, Cat# 40203D) at a bead to T cell ratio of 3:1 in cell culture media X-VIVO 15 (Lonza, Cat# BE02–060Q) with 100 U/mL IL2 and 5% human AB serum (Millipore Sigma, Cat# H5667) in tissue culture wells. After 24 hours, Dynabeads CD3/CD28 were removed from cultured T cells and activated T cells were continued to be cultured for 1 week. At the end of culture, cells were harvested and cryopreserved in LN2 for use in the indicated assays.

NK cell–cytotoxicity assay

To assess cytotoxicity, cryopreserved NK cells were thawed and co-cultured with A549 or H460 NSCLC lines at the indicated E:T ratios. The cytotoxicity was measured by Real-Time Cell Analysis (RTCA) as previously described (15). Briefly, target cells (5000 cells/well) were plated and cultured in an xCELLigence RTCA instrument (Agilent Technologies, Inc) installed in a CO₂ incubator. Impedance measurements are automatically recorded at 15-minute intervals and plotted by the xCELLigence software using the dimensionless parameter known as cell index (CI). After overnight incubation, sIL15_TRACK NK and control NK cells were added into the E-plate and co-cultured for at least an additional 40 hours. The normalized cell index was the relative cell impedance presented in the percentage of the value at the base-time. The cytotoxicity of effector cells was calculated with the following equation: % of cytolysis = $(CI_{no\ effector} - CI_{effector}) / CI_{no\ effector} \times 100$.

Enzyme-linked immunosorbent assay (ELISA)

The concentration of human IL15 was measured in triplicate in culture medium on the day of cell harvesting according to the manufacturer's instructions (R&D, Cat# S1500).

Cryopreserved NK cells were thawed and cultured (1×10^6 /mL) with A549 or H460 NSCLC cells at an E:T of 5:1 in RPMI 1640 medium supplemented with 10% FBS in the absence of any cytokines for 48 hours. The concentrations of IFN- γ (R&D, Cat# DY285B-05), TNF- α (R&D, Cat# DY210-05), and granzyme B (GZMB) (R&D, Cat# DY2906-05) in the supernatants were measured according to the manufacturer's manuals in triplicate.

Flow cytometry

For cell surface staining, cells to be tested (e.g., NK cells) were first resuspended in FACS buffer composed of PBS (Gibco, Cat# 10010023), 2 mM EDTA (Invitrogen, Cat# 15575020) and 2% FBS, followed by staining with the indicated antibodies at 4°C for 20 minutes avoiding the light. Cells were next washed twice with FACS buffer, and subject to flow cytometric analysis using a Fortessa X20 (BD Biosciences). All flow cytometry antibodies are listed in Supplementary Table S1. Data were analyzed using FlowJo V10 software.

Vector Copy Number

Briefly, DNA was isolated from sIL15-TRACK NK cells by using QIAamp DNA Mini Kit (Qiagen, Cat# 51304). A quantitative polymerase chain reaction (qPCR) assay was performed to detect vector DNA, using CFX 96 real-time PCR Detection System. The primer sequences were tEGFR_F, 5'-TCC GGA TTA GTC CAA TTT GTT AAA G-3' and tEGFR_R, 5'-TCT ATG GCT CGT ACT CTA TAG GC-3'. The standard samples were serial 10-fold dilutions of a known copy number. The results were normalized and expressed as genome equivalent copies per NK cell.

NSG xenograft models

Adult NOD/SCID IL2R γ null (NSG) mice (8–12 weeks old) were purchased from the Jackson Laboratory and housed at the animal facility of City of Hope. On day -1, NSG mice were inoculated intravenously (i.v.) with FFLuc-labeled A549 or H460 NSCLC cell lines. The A549 cell line used for the establishment of NSCLC and assessment of antitumor efficacy is what is classically termed an experimental or artificial metastasis model (16). On day 0, according to the treatment regimens, the mice received an i.v. infusion of different treatments including vehicle (PBS), NT NK cells, sIL15 NK cells, NT_TRACK NK cells or sIL15_TRACK NK cells without or with atezolizumab administered i.v. or intraperitoneally (i.p.) which was provided by the City of Hope National Medical Center Pharmacy. In one set of experiments, human T cells obtained from normal donors were activated and expanded as noted above (see NK-cell and T-cell isolation and expansion) and were infused on day 0. Tumor growth was monitored by bioluminescence imaging (BLI) over time. Briefly, 3 mg D-Luciferin Firefly (Biosynth International, Cat# L-8220) was given by i.p. injection into each mouse. After 1 minute, mice were anesthetized by gas anesthesia (3% isoflurane) and placed on to a black imaging chamber. Imaging was acquired by *in vivo* imaging system

(IVIS) (Spectral Instruments Imaging) and analyzed via Aura software (Spectral Instruments Imaging). All mice were euthanized by CO₂ inhalation when they reached the endpoint of an experiment. Anti-coagulated blood and sera were collected for complete blood count (CBC) and chemistries, respectively. Tissues including lung, spleen and liver were harvested and prepared as formalin-fixed, paraffin-embedded (FFPE) blocks for pathologic assessment. In the sense that our experimental design was to engraft NSG mice with human tumors and assess the antitumor activity of human NK cells or human NK cells plus human T cells against the human tumors, we referred to these studies as allogeneic in nature as opposed to xenogeneic.

NSG mice (8–12 weeks old) were also used to evaluate the toxicity and safety of sIL15_TRACK NK cells. On day 0, the mice received different treatments: vehicle (PBS) or sIL15_TRACK NK cells (from 2 different human UCBs) without or with i.v. atezolizumab. Body weight and body temperature were monitored weekly on days 7, 14, 21, and 28. Mice from each group were euthanized by CO₂ inhalation on days 7, 14, and 28. Anti-coagulated blood and sera were collected for CBC, chemistries and cytokine analysis, respectively. Human NK cells were quantified in mouse blood by flow cytometry as positive for co-expression of human CD45⁺ and human CD56⁺. Tissues including lung, spleen and liver were harvested and prepared as FFPE blocks for pathologic analysis.

All CBC, chemistries and cytokine analysis were performed by IDEXX BioAnalytics.

Immunohistochemistry

Tissues collected and processed for histopathological evaluation were fixed in 10% neutral buffered formalin, embedded in paraffin, sectioned at 5µm, and stained with Modified Mayer's Hematoxylin (American MasterTech Scientific, Cat# HXMMHLT) and Eosin Y (American MasterTech Scientific, Cat# STE0250) on Tissue-Tek Prisma Plus automated slide stainer (Sakura Finetek USA) following the standard laboratory protocol at City of Hope Pathology Core.

IHC staining was performed on Ventana Discovery Ultra IHC research platform (Roche Diagnostics) following the standard laboratory protocol at the City of Hope Pathology Core. Tissue blocks were cut into 5-µm-thick sections, de-paraffinized, rehydrated, and treated by endogenous peroxidase activity inhibition and antigen retrieval with Cell conditioning 1 buffer (Roche Diagnostics, Cat# 950124). The primary antibody rabbit anti-NCR1/NKP46 (Abcam, Cat# ab224703) was used at the concentration of 3.46µg/mL. The staining was visualized by DISCOVERY ChromoMap DAB Detection system (Roche Diagnostics) and counterstained with Modified Mayer's Hematoxylin. Appropriate positive and negative controls were employed for each run of IHC staining. All histopathological and immunohistochemical analyses were performed using an Olympus BX46 microscope by a pathologist and images were captured and acquired using an Olympus DP27 digital camera and cellSens Standard V2.2 software (Olympus Life Science).

Statistical analysis

All data presented in the figures of this study received statistical review both at the time of planning the experiment and once completed. *P* values are only indicated where

statistical differences were obtained. Continuous data/endpoints were summarized by mean and standard error of mean (SEM). Student *t* test or paired *t* test were used to compare two independent or paired groups. One-way ANOVA model was used for multiple-group comparisons. Linear mixed models, or one-way or two-way ANOVA with repeated measures by GraphPad Prism, were used to assess the group difference based on the variance-covariance structure due to repeated measures (e.g., tumor growth over time) or matched groups (e.g., same donors). Overall survival data were analyzed by Kaplan–Meier method for survival function estimation and log-rank test for group comparison. For multiple-group comparisons, *p* values were adjusted by Holm–Sidak method. *P* values ≤ 0.05 were considered statistically significant. Statistical software, including GraphPad Prism 9.0 and SAS 9.4, were used for data analysis.

Data availability

The data generated in this study are available within the article and supplementary data files or upon reasonable request to the corresponding authors.

Results

Generation of sIL15_TRACK NK cells

As shown in Figure 1A, sIL15_TRACK NK cells consistently expanded *ex vivo* over an average of 1,000-fold in 17 days including two batches of sIL15_TRACK NK cells produced under Good Manufacturing Practice (GMP) (Supplementary Fig. S1A). The average purity of the sIL15_TRACK NK cell product was 98.5%, with $< 0.5\%$ T-cell contamination, and was similar in the NT NK cells, NT_TRACK NK cells, and sIL15 NK cells (Fig. 1B). More than 75% of sIL15_TRACK NK cells expressed PD-L1 following overnight incubation in IL12 and IL18, with over 50% transduction efficiency of sIL15 which was determined by the co-expression of tEGFR (Fig. 1C and Supplementary Fig. S1B).

To assess the secretion of IL15 by sIL15_TRACK NK cells, IL15 concentrations were measured in the culture media supernatant on day 17. sIL15_TRACK NK cells secreted significantly more IL15 (mean, 39.7 pg/ml; range 28.3–66.9 pg/ml) compared to sIL15 NK cells (mean, 5.3 pg/ml; range 3.8–8.1 pg/ml), while NT NK cells and NT_TRACK NK cells secreted undetectable levels of IL15 regardless of PD-L1 expression (Fig. 1D). With regards to the safety of retroviral transduction, vector copy number (VCN) within the sIL15_TRACK NK-cell product, generated with our manufacturing standard operating procedure (SOP), was consistently assessed at < 5 copies per transduced cell (Fig. 1E). Following cryopreservation, sIL15_TRACK NK cells demonstrated high recovery (mean, 87.5%) and viability (mean, 83.9%) (Fig. 1F). To investigate the possibility that the IL15-encoding gene in the vector may result in autonomous or dysregulated growth of NK cells, we cultured sIL15_TRACK NK cells in media without any cytokines for 42 days. Cultured sIL15_TRACK NK cells did not show any signs of abnormal growth during the 6-week experiment, as assessed by the number of viable cells in the culture, even when co-cultured with irradiated NSCLC (A549) cells (Fig. 1G).

***In vitro* functional activity of sIL15-TRACK NK cells**

When testing NK-cell cytotoxic activity against human NSCLC cell lines (A549 or H460) *in vitro* using the RTCA, sIL15_TRACK NK cells lysed the NSCLC cells more efficiently than the control groups of NT NK, NT_TRACK NK, and sIL15 NK at different E: T ratios (Fig. 2A-B and Supplementary Fig. S2A-B). A549 or H460 NSCLC cells that were cocultured with sIL15_TRACK NK cells grew significantly slower than cells cocultured with the control groups of NK cells (Fig. 2C). To assess cytokine and granzyme production by sIL15_TRACK NK cells, levels of IFN- γ , TNF- α and granzyme B (GZMB) were measured in the supernatant 48 hours after NK cells were co-cultured with A549 or H460 NSCLC cells. sIL15_TRACK NK cells secreted significantly higher levels of IFN- γ and TNF- α compared with NT_TRACK NK cells, while NT NK cells and sIL15 NK cells barely secreted IFN- γ or TNF- α (Fig. 2D). sIL15_TRACK NK cells consistently produced significantly higher levels of GZMB when cocultured with NSCLC cells compared to all three control groups (Fig. 2D). In our previous study, we observed that the expression of CD69 and CD25 was significantly increased on PD-L1⁺ NK cells compared with PD-L1⁻ NK cells (14). Consistent with this, sIL15_TRACK NK cells displayed increased expression of activation receptors, including CD69, CD25 and TRAIL, as well as increased expression of the inhibitory receptor NKG2A, when compared to sIL15 NK cells (Fig. 2E and Supplementary Fig. S2C-D). However, there was no significant difference in the expression of CD16, NKG2D, NKp30, NKp44, DNAM-1, CD94, and KIR-NKAT2 between sIL15 NK cells and sIL15_TRACK NK cells (Supplementary Fig. S2E).

***In vivo* functional activity of sIL15_TRACK NK cells**

Using an experimental metastatic mouse model of A549 NSCLC (Fig. 3A), we next investigated whether adoptive transfer of sIL15_TRACK NK cells could control tumor progression better than the control groups of NK cells. First, mice were inoculated with A549 NSCLC cells (0.2×10^6 /mouse) on day -1, followed by i.v. infusions of NK cells (1×10^7 /mouse) consisting of either (1) vehicle, (2) NT NK, (3) sIL15 NK, or (4) sIL15_TRACK NK cells on days 0, 2, 5, 7 and 12. Tumor burden, monitored by BLI, was significantly lower in the group treated with sIL15_TRACK NK cells compared to the three control groups (Fig. 3B-C). Next, to optimize the adoptive transfer dose, mice received four i.v. infusions of sIL15_TRACK NK cells at three different doses (5×10^6 /mouse, 1×10^7 /mouse, or 2×10^7 /mouse) under identical schedules of administration (Fig. 3D). We found that infusion of 1×10^7 sIL15_TRACK NK cells provided significantly better tumor control than 5×10^6 sIL15_TRACK NK cells, but a dose of 2×10^7 sIL15_TRACK NK cells offered no better control than 1×10^7 sIL15_TRACK NK cells (Fig. 3E-F). The number of metastatic tumor nodules in the lung decreased significantly in all groups receiving NK cells compared to the group treated with vehicle only, and mice infused with 1×10^7 or 2×10^7 sIL15_TRACK NK cells had significantly fewer metastatic tumor nodules compared to those infused with 5×10^6 sIL15_TRACK NK cells but there was no significant difference between the group infused with 1×10^7 and 2×10^7 sIL15_TRACK NK cells (Fig. 3G). Regarding human NK-cell persistence *in vivo*, the group treated with 2×10^7 sIL15_TRACK NK cells showed the highest percentage of human NK cells in mice lung, spleen, and liver on day 21 (15 days after the final infusion) compared to mice infused with 5×10^6 or 1×10^7 sIL15_TRACK NK cells (Fig. 3H and Supplementary Fig. S3A-B),

suggesting that *in vivo*, NK cells secreting sIL15 persist in tissues in a dose-dependent manner.

Using the same tumor-bearing mice from the experiment described above, we also investigated toxicity and safety. On day 21, analysis of complete blood counts (CBC), chemistries, and cytokine profiling were performed. As shown in Supplementary Fig. S3C, the following analyses did not have statistically significant differences in the three NK-cell treatment groups compared with the vehicle control group: neutrophil (NEU), lymphocyte (LYM), red blood cell (RBC), hemoglobin (HGB) and platelet (PLT); while white blood cells (WBC) increased significantly in mice treated with 2×10^7 sIL15_TRACK NK cells compared to the vehicle control group. Regarding chemistries, no significant increase was noted in the three NK cell-treatment groups compared to the vehicle group, including alanine aminotransferase (ALT), aspartate aminotransferase (AST), alkaline phosphatase (ALP), creatine kinase (CK), albumin (ALB) and blood urea nitrogen (BUN) (Supplementary Fig. S3D). In the cytokine profiling analyses, the following cytokine concentrations were not significantly different across all four treatment groups: hIL15, hIFN γ , hTNF α , mouse (m) IFN γ , mL6, and mL1 β (Supplementary Fig. S3E).

To assess sIL15_TRACK NK cells in a second NSCLC tumor model, we utilized a more aggressive metastatic mouse model with the NSCLC cell line H460 (17), which provides a lethal endpoint in order to assess survival. Vehicle (PBS), NT NK cells, sIL15 NK cells, and sIL15_TRACK NK cells were each evaluated in this model (Supplementary Fig. S4A). Following the infusion of only five doses over 12 days, sIL15_TRACK NK cells were able to significantly improve suppression of tumor progression compared to other three treatment groups (Fig. 4A-B), along with a significant extension of overall survival (Fig. 4C).

***In vivo* functional activity of sIL15_TRACK NK cells combined with atezolizumab**

We previously demonstrated that atezolizumab directly activates PD-L1⁺ NK cells via the p38–NF κ B pathway (14), and others have shown it can activate T cells following ICB (18); even more so in the presence of IL15 (19). To assess whether the addition of atezolizumab could further increase the antitumor efficacy of sIL15_TRACK NK cells, and to assess if the addition of human T cells could further enhance such effects, we designed an experiment where all mice in the study were engrafted with A549 NSCLC on day –1 and on day 0 received a single infusion of 2×10^6 normal, activated T cells in combination with either vehicle (PBS), atezolizumab, sIL15_TRACK NK cells, or sIL15_TRACK NK cells plus atezolizumab (Supplementary Fig. S4B). Considering the potential for acute GvHD induced by activated xenogeneic T cells, this experiment was performed using only 2×10^6 human T cells, which is much lower than the previously reported threshold for the onset of acute GvHD (20). Among each of these combinations, the group of mice treated with the combination of T cells and sIL15_TRACK NK cells plus atezolizumab showed the best suppression of tumor growth (Fig. 4D-E).

Safety evaluation of sIL15_TRACK NK cells

Lastly, we evaluated the safety of sIL15_TRACK NK cells in 60 mice (30 females, 30 males) divided into three treatment groups: vehicle control, sIL15_TRACK NK cells,

and sIL15_TRACK NK cells plus atezolizumab. The mice received intravenous injections of sIL15_TRACK NK cells (1×10^7 /mouse) on days 0, 2, 4 and 6 with or without atezolizumab (2 mg). Each group treated with sIL15_TRACK NK cells included cells from two different donors, one of which was a GMP-grade sIL15_TRACK NK-cell product. No mice were engrafted with NSCLC tumors for these toxicity and safety studies. Mice within each group were euthanized at different time points for analysis: early - day 7; middle - day 14; and end - day 28. CBC, chemistries, cytokine profiling, and histopathology were evaluated at each time point. Throughout the study, body weight and temperature were monitored and recorded each week (Fig. 5A).

Overall, as shown in Figure 5B, body weights and body temperatures did not show any significant differences between any of the groups. While assessing sIL15_TRACK NK cell persistence *in vivo*, our data showed both the highest percentage and absolute numbers of hCD45⁺hCD56⁺ cells in blood on day 7 (24 hours post all NK-cell infusions) when compared to those on day 14 (8 days post all NK-cell infusions), and day 28 (22 days post all NK-cell infusions) (Fig. 5C-D), indicating sIL15_TRACK NK cells were not proliferating autonomously *in vivo*, consistent with our *in vitro* results noted earlier (Fig. 1G).

We also assessed CBCs, blood chemistries, and serum cytokine levels at different time points to provide more information about the safety of the sIL15_TRACK NK cells product in the absence or presence of atezolizumab. At the earliest time point (day 7), when the human NK-cell population was the highest in mice, white blood-cell lineages (WBC, NEU and LYM), red blood-cell parameters (RBC and HGB) and platelets did not show any differences among the groups (Fig. 5E). Similar findings were seen for the liver function parameters (ALT, AST, ALP) and kidney function parameters (CK, ALB, BUN) (Fig. 5F). With regards to the cytokine profiling, the following analyses did not show statistically significant differences among any of the three groups: hTNF α , mIFN γ , mIL6, and mIL1 β ; however, concentrations of hIL15 and hIFN γ were significantly higher in groups treated with sIL15_TRACK NK cells regardless of the presence or absence of atezolizumab compared to those mice treated with vehicle alone (Fig. 5G). At the middle time point of day 14, there were no significant differences in CBC and chemistries among the different groups, while concentrations of hIL15 and hIFN γ were significantly higher in the group treated with sIL15_TRACK NK cells only compared to those mice treated with vehicle alone (Supplementary Fig. S5A-C). Furthermore, we did not observe any significant differences in CBC, chemistries, or cytokine profiling at the end time point of day 28 (Supplementary Fig. S5D-F). Similarly, there was no evidence of tissue damage including damage to the lung, liver, and spleen in mice post sIL15_TRACK NK cell infusions in the presence or absence of atezolizumab treatment on day 28 (Supplementary Fig. S6). Altogether, these data demonstrate that the administration of sIL15_TRACK NK cells with or without atezolizumab appears safe and does not induce toxicity in this animal model.

Discussion

PD-L1 expression has been extensively reported on tumor cells, as well as on immune cells such as macrophages (21), T cells (22), and NK cells (23). In our previous study, we found

PD-L1 expression on primary human NK cells after recognizing and responding to tumor cells or following stimulation with cytokines IL12, IL18 and IL15 (14). We also observed that CD69 and CD25 were significantly increased on PD-L1⁺ NK cells compared to PD-L1⁻ NK cells, while the expression of CD94, KLRG1, NKp44, and NKG2D showed no significant difference between these two subsets. To understand the functional significance of PD-L1⁺ NK cells, previously, we used a human leukemia completely void of PD-L1 and demonstrated that atezolizumab can directly activate these PD-L1⁺ NK cells and enhance their ability to control liquid tumor cell growth *in vivo*. We referred to these cells as tumor responsive and cytokine-activated killer (TRACK) NK cells.

Cellular immunotherapy with NK cells has shown some promise in the treatment of hematologic malignancies, but thus far success has been elusive in the arena of solid tumors. One challenge faced when using NK cells is their ability to successfully traffic into tumor beds and penetrate the barriers imposed by solid tumors (24). However, in our study, immunohistochemical staining showed sIL15_TRACK NK cells detectable in mouse lung two weeks after final infusion in a dose-dependent manner. Cells were also detectable liver, suggesting that sIL15_TRACK NK cells are able to traffic to solid tumor sites in these and other organs as demonstrated in our study assessing PSCA CAR NK cells in models of metastatic pancreatic cancer (25).

As is now widely accepted, solid tumors such as NSCLC can evade the host immune system by expressing PD-L1, which in part suppresses T cell-mediated antitumor responses. Anti-PD-L1 therapies such as atezolizumab block PD-L1/PD-1 interactions and restore immune cell function. Preclinical studies have demonstrated that anti-PD-L1 therapy can enhance the activity of T cells in the tumor microenvironment, leading to reduced tumor burden and increased survival (26,27), and we demonstrated that atezolizumab can have a similar antitumor effect by acting directly on PD-L1⁺ NK cells (14). Here we show that atezolizumab can enhance tumor control *in vivo* when given in combination with activated T cells and sIL15_TRACK NK cells, compared to activated T cells plus atezolizumab or activated T cells plus sIL15_TRACK NK cells alone. When using murine colon adenocarcinoma (MC38) and murine lymphoma (A20) models, Tang *et al.* observed that anti-PD-L1 could accumulate in tumor tissues regardless of PD-L1 expression on tumor cells (28). Thus, additional studies will be needed to determine the exact mechanism(s) of action of atezolizumab in our experimental setting.

Although NK cells are classically referred to as innate immune cells, they share many properties with adaptive lymphocytes, particularly CD8⁺ T cells. These include a common lymphoid progenitor, surface markers, and secretion of perforin and granzymes to mediate cytotoxicity (29,30). Recent studies have also described “memory-like” properties of NK cells, with evidence for virus-induced memory NK cells, cytokine-induced memory NK cells, and liver-restricted memory NK cells (31). Yokoyama and colleagues found that pre-activating mouse NK cells with IL12, IL15, and IL18 generated cells that they defined as memory-like NK cells. These cells exhibited enhanced responses upon restimulation with cytokines after adoptive transfer into naïve Rag1^{-/-} mice, compared to NK cells activated with IL15 alone (32). Pre-activation also resulted in enhanced mouse NK-cell accumulation, persistence, and effector function in tumor tissue (33). Similarly, human

IL12, IL15, and IL18-induced memory-like NK cells have better expansion and antitumor activity in response to exogenous IL2 after adoptive transfer into immunodeficient mice (34). Memory-like NK cells express upregulated inhibitory or activating receptors including NKG2A, NKp30, NKp44, NKp46, NKG2D, CD62L, and CD25, whereas other receptors such as KIR, CD57, NKG2C, DNAM-1, CD137, and CD11b appear unchanged (or in the case of NKp80, decreased) (34,35). Given that the *ex vivo* preparation of PD-L1⁺ cells that we first discovered *in vivo* undergoes comparable cytokine-induced activation *ex vivo*, our sIL15_TRACK NK cells likely have memory-like properties as described.

In previous work we demonstrated that *ex vivo* expanded human NK cells lacking endogenous IL15 secretion could not survive beyond a few days *in vivo*, whereas engineered NK cells that secrete soluble IL15 had much better persistence (15). Similarly, mice treated with anti-CD19 CAR NK cells expressing IL15 had higher frequencies of CAR NK cells in blood, bone marrow, liver, and spleen, and had greater persistence compared to mice treated with conventional anti-CD19 CAR NK cells (36). Although IL15 promotes proliferation, development, and antitumor activity of NK cells, its systemic infusion, especially at high doses, is associated with considerable toxicity including weight loss and skin rash (37–39). Additionally, in a study of an IL15 superagonist that is formed by combining IL15 and soluble IL15R α , Guo *et al.* found that treatment of mice with IL15 superagonist resulted in systemic physiologic dysfunction including hypothermia, weight loss, and acute liver injury that was partially reversed by NK-cell depletion (40). Conlon *et al.* also showed that IL15 treatment could clear pulmonary lesions in patients with malignant melanoma, but treatment caused side effects including liver injury, fever, and thrombocytopenia (41). In a Phase I clinical trial of continuous intravenous infusion of rhIL15 to treat solid tumors, eight of twenty-seven adult patients had serious adverse events and two patients died (42). Finally, Christodoulou and colleagues recently reported that CAR-NK cells engineered to secrete IL15 caused early mortality in mice engrafted with MV-4–11 cells. Their model was associated with high numbers of infiltrating NK cells that increased levels of systemic soluble IL15 and high levels of human TNF- α (43). However, in the current study we evaluated the safety of our sIL15_TRACK NK cells in mice either with or without tumor engraftment. The frequencies and absolute numbers of sIL15_TRACK NK cells decreased gradually post infusion and we did not observe any significant changes in body weight, temperature, CBC, liver function, kidney function, or cytokine profile, suggesting our cell product has a lower probability of causing systemic toxicity and is an encouraging candidate to move forward into human studies. Of note, a sizeable fraction of the *ex vivo* expanded TRACK NK cells utilized in our studies did not undergo successful transduction with sIL15 yet are infused along with the sIL15_TRACK NK cells. These non-transduced PD-L1⁺ NK cells still require IL15 for survival *in vivo* and thus likely serve as an important “sink”, helping prevent higher doses of IL15 being released into the systemic circulation following infusion.

In summary, in the current study, we activated, expanded, and retrovirally transduced UCB NK cells with sIL15 and subsequently induced PD-L1 expression through cytokine activation. These sIL15_TRACK NK cells expressed significantly higher levels of NKG2A, CD25, CD69, and TRAIL, and demonstrated better killing of solid tumor cell targets compared to similarly prepared NK cells lacking either sIL15 or PD-L1 expression. Further,

we demonstrated that the cryopreserved, allogeneic off-the-shelf sIL15_TRACK NK cells can traffic to the lungs, survive for weeks *in vivo*, are non-toxic at efficacious doses, and can slow tumor progression and improve survival of mice bearing NSCLC tumor cells through direct cytotoxic activity. We also demonstrated that when combined with T cells and the anti-PD-L1 atezolizumab, sIL15_TRACK NK cells exhibit superior suppression of NSCLC growth *in vivo* compared to activated T cells plus atezolizumab or activated T cells plus sIL15_TRACK NK cells alone. Collectively, these preclinical results have supported the initiation of a Phase I clinical trial with sIL15_TRACK NK cells without or with atezolizumab in patients with relapsed and refractory NSCLC (NCT05334329).

Supplementary Material

Refer to Web version on PubMed Central for supplementary material.

Acknowledgments:

This work was supported by grants from the NIH (CA266457, NS106170, CA247550, CA163205, CA265095, CA210087, and CA163205).

Drs. Caligiuri and Yu are co-founders and shareholders of CytoImmune Therapeutics, Inc. Dr. Mansour is a shareholder in CytoImmune Therapeutics.

Funding information:

This work was supported by grants from the NIH (CA266457, CA210087, CA265095, CA163205, NS106170, AI129582, CA247550, CA264512, and CA223400).

References

1. Herbst RS, Heymach JV, Lippman SM. Lung cancer. *N Engl J Med* 2008;359(13):1367–80 doi 10.1056/NEJMra0802714. [PubMed: 18815398]
2. Akinboro O, Larkins E, Pai-Scherf LH, Mathieu LN, Ren Y, Cheng J, et al. FDA Approval Summary: Pembrolizumab, Atezolizumab, and Cemiplimab-rwlc as single agents for first-line treatment of advanced/metastatic PD-L1 high NSCLC. *Clin Cancer Res* 2022 doi 10.1158/1078-0432.CCR-21-3844.
3. Gandhi L, Rodriguez-Abreu D, Gadgeel S, Esteban E, Felip E, De Angelis F, et al. Pembrolizumab plus Chemotherapy in Metastatic Non-Small-Cell Lung Cancer. *N Engl J Med* 2018;378(22):2078–92 doi 10.1056/NEJMoa1801005. [PubMed: 29658856]
4. Herbst RS, Giaccone G, de Marinis F, Reinmuth N, Vergnenegre A, Barrios CH, et al. Atezolizumab for First-Line Treatment of PD-L1-Selected Patients with NSCLC. *N Engl J Med* 2020;383(14):1328–39 doi 10.1056/NEJMoa1917346. [PubMed: 32997907]
5. Paz-Ares L, Luft A, Vicente D, Tafreshi A, Gumus M, Mazieres J, et al. Pembrolizumab plus Chemotherapy for Squamous Non-Small-Cell Lung Cancer. *N Engl J Med* 2018;379(21):2040–51 doi 10.1056/NEJMoa1810865. [PubMed: 30280635]
6. Reck M, Mok TSK, Nishio M, Jotte RM, Cappuzzo F, Orlandi F, et al. Atezolizumab plus bevacizumab and chemotherapy in non-small-cell lung cancer (IMpower150): key subgroup analyses of patients with EGFR mutations or baseline liver metastases in a randomised, open-label phase 3 trial. *Lancet Respir Med* 2019;7(5):387–401 doi 10.1016/S2213-2600(19)30084-0. [PubMed: 30922878]
7. Socinski MA, Jotte RM, Cappuzzo F, Orlandi F, Stroyakovskiy D, Nogami N, et al. Atezolizumab for First-Line Treatment of Metastatic Nonsquamous NSCLC. *N Engl J Med* 2018;378(24):2288–301 doi 10.1056/NEJMoa1716948. [PubMed: 29863955]

8. West H, McCleod M, Hussein M, Morabito A, Rittmeyer A, Conter HJ, et al. Atezolizumab in combination with carboplatin plus nab-paclitaxel chemotherapy compared with chemotherapy alone as first-line treatment for metastatic non-squamous non-small-cell lung cancer (IMpower130): a multicentre, randomised, open-label, phase 3 trial. *Lancet Oncol* 2019;20(7):924–37 doi 10.1016/S1470-2045(19)30167-6. [PubMed: 31122901]
9. Yu Y, Zeng D, Ou Q, Liu S, Li A, Chen Y, et al. Association of Survival and Immune-Related Biomarkers With Immunotherapy in Patients With Non-Small Cell Lung Cancer: A Meta-analysis and Individual Patient-Level Analysis. *JAMA Netw Open* 2019;2(7):e196879 doi 10.1001/jamanetworkopen.2019.6879.
10. Chang CH, Qiu J, O’Sullivan D, Buck MD, Noguchi T, Curtis JD, et al. Metabolic Competition in the Tumor Microenvironment Is a Driver of Cancer Progression. *Cell* 2015;162(6):1229–41 doi 10.1016/j.cell.2015.08.016. [PubMed: 26321679]
11. Vivier E, Raulet DH, Moretta A, Caligiuri MA, Zitvogel L, Lanier LL, et al. Innate or adaptive immunity? The example of natural killer cells. *Science* 2011;331(6013):44–9 doi 10.1126/science.1198687. [PubMed: 21212348]
12. Asai O, Longo DL, Tian ZG, Hornung RL, Taub DD, Ruscetti FW, et al. Suppression of graft-versus-host disease and amplification of graft-versus-tumor effects by activated natural killer cells after allogeneic bone marrow transplantation. *J Clin Invest* 1998;101(9):1835–42 doi 10.1172/JCI1268. [PubMed: 9576746]
13. Ruggeri L, Capanni M, Urbani E, Perruccio K, Shlomchik WD, Tosti A, et al. Effectiveness of donor natural killer cell alloreactivity in mismatched hematopoietic transplants. *Science* 2002;295(5562):2097–100 doi 10.1126/science.1068440. [PubMed: 11896281]
14. Dong W, Wu X, Ma S, Wang Y, Nalin AP, Zhu Z, et al. The Mechanism of Anti-PD-L1 Antibody Efficacy against PD-L1-Negative Tumors Identifies NK Cells Expressing PD-L1 as a Cytolytic Effector. *Cancer Discov* 2019;9(10):1422–37 doi 10.1158/2159-8290.CD-18-1259. [PubMed: 31340937]
15. Lu T, Ma R, Dong W, Teng KY, Kollath DS, Li Z, et al. Off-the-shelf CAR natural killer cells secreting IL-15 target spike in treating COVID-19. *Nat Commun* 2022;13(1):2576 doi 10.1038/s41467-022-30216-8. [PubMed: 35546150]
16. Fidler IJ, Kripke ML. Metastasis results from preexisting variant cells within a malignant tumor. *Science* 1977;197(4306):893–5 doi 10.1126/science.887927. [PubMed: 887927]
17. Townsend MH, Anderson MD, Weagel EG, Velazquez EJ, Weber KS, Robison RA, et al. Non-small-cell lung cancer cell lines A549 and NCI-H460 express hypoxanthine guanine phosphoribosyltransferase on the plasma membrane. *Onco Targets Ther* 2017;10:1921–32 doi 10.2147/OTT.S128416. [PubMed: 28408844]
18. Mohan N, Hosain S, Zhao J, Shen Y, Luo X, Jiang J, et al. Atezolizumab potentiates Tcell-mediated cytotoxicity and coordinates with FAK to suppress cell invasion and motility in PD-L1(+) triple negative breast cancer cells. *Oncoimmunology* 2019;8(9):e1624128 doi 10.1080/2162402X.2019.1624128.
19. Yu P, Steel JC, Zhang M, Morris JC, Waitz R, Fasso M, et al. Simultaneous inhibition of two regulatory T-cell subsets enhanced Interleukin-15 efficacy in a prostate tumor model. *Proc Natl Acad Sci U S A* 2012;109(16):6187–92 doi 10.1073/pnas.1203479109. [PubMed: 22474386]
20. Nervi B, Rettig MP, Ritchey JK, Wang HL, Bauer G, Walker J, et al. Factors affecting human T cell engraftment, trafficking, and associated xenogeneic graft-vs-host disease in NOD/SCID beta2mnull mice. *Exp Hematol* 2007;35(12):1823–38 doi 10.1016/j.exphem.2007.06.007. [PubMed: 17764813]
21. Hartley GP, Chow L, Ammons DT, Wheat WH, Dow SW. Programmed Cell Death Ligand 1 (PD-L1) Signaling Regulates Macrophage Proliferation and Activation. *Cancer Immunol Res* 2018;6(10):1260–73 doi 10.1158/2326-6066.CIR-17-0537. [PubMed: 30012633]
22. Latchman YE, Liang SC, Wu Y, Chernova T, Sobel RA, Klemm M, et al. PD-L1-deficient mice show that PD-L1 on T cells, antigen-presenting cells, and host tissues negatively regulates T cells. *Proc Natl Acad Sci U S A* 2004;101(29):10691–6 doi 10.1073/pnas.0307252101. [PubMed: 15249675]

23. Terme M, Ullrich E, Aymeric L, Meinhardt K, Coudert JD, Desbois M, et al. Cancer-induced immunosuppression: IL-18-elicited immunoablative NK cells. *Cancer Res* 2012;72(11):2757–67 doi 10.1158/0008-5472.CAN-11-3379. [PubMed: 22427351]
24. Biederstadt A, Rezvani K. Engineering the next generation of CAR-NK immunotherapies. *Int J Hematol* 2021;114(5):554–71 doi 10.1007/s12185-021-03209-4. [PubMed: 34453686]
25. Teng KY, Mansour AG, Zhu Z, Li Z, Tian L, Ma S, et al. Off-the-Shelf Prostate Stem Cell Antigen-Directed Chimeric Antigen Receptor Natural Killer Cell Therapy to Treat Pancreatic Cancer. *Gastroenterology* 2022;162(4):1319–33 doi 10.1053/j.gastro.2021.12.281. [PubMed: 34999097]
26. Tumeh PC, Harview CL, Yearley JH, Shintaku IP, Taylor EJ, Robert L, et al. PD-1 blockade induces responses by inhibiting adaptive immune resistance. *Nature* 2014;515(7528):568–71 doi 10.1038/nature13954. [PubMed: 25428505]
27. Akbay EA, Koyama S, Carretero J, Altabef A, Tchaicha JH, Christensen CL, et al. Activation of the PD-1 pathway contributes to immune escape in EGFR-driven lung tumors. *Cancer Discov* 2013;3(12):1355–63 doi 10.1158/2159-8290.CD-13-0310. [PubMed: 24078774]
28. Tang H, Liang Y, Anders RA, Taube JM, Qiu X, Mulgaonkar A, et al. PD-L1 on host cells is essential for PD-L1 blockade-mediated tumor regression. *J Clin Invest* 2018;128(2):580–8 doi 10.1172/JCI96061. [PubMed: 29337303]
29. Kondo M, Weissman IL, Akashi K. Identification of clonogenic common lymphoid progenitors in mouse bone marrow. *Cell* 1997;91(5):661–72 doi 10.1016/s0092-8674(00)80453-5. [PubMed: 9393859]
30. Sun JC, Lanier LL. NK cell development, homeostasis and function: parallels with CD8(+) T cells. *Nat Rev Immunol* 2011;11(10):645–57 doi 10.1038/nri3044. [PubMed: 21869816]
31. Min-Oo G, Kamimura Y, Hendricks DW, Nabekura T, Lanier LL. Natural killer cells: walking three paths down memory lane. *Trends Immunol* 2013;34(6):251–8 doi 10.1016/j.it.2013.02.005. [PubMed: 23499559]
32. Cooper MA, Elliott JM, Keyel PA, Yang L, Carrero JA, Yokoyama WM. Cytokine-induced memory-like natural killer cells. *Proc Natl Acad Sci U S A* 2009;106(6):1915–9 doi 10.1073/pnas.0813192106. [PubMed: 19181844]
33. Ni J, Miller M, Stojanovic A, Garbi N, Cerwenka A. Sustained effector function of IL-12/15/18-preactivated NK cells against established tumors. *J Exp Med* 2012;209(13):2351–65 doi 10.1084/jem.20120944. [PubMed: 23209317]
34. Leong JW, Chase JM, Romee R, Schneider SE, Sullivan RP, Cooper MA, et al. Preactivation with IL-12, IL-15, and IL-18 induces CD25 and a functional high-affinity IL-2 receptor on human cytokine-induced memory-like natural killer cells. *Biol Blood Marrow Transplant* 2014;20(4):463–73 doi 10.1016/j.bbmt.2014.01.006. [PubMed: 24434782]
35. Romee R, Rosario M, Berrien-Elliott MM, Wagner JA, Jewell BA, Schappe T, et al. Cytokine-induced memory-like natural killer cells exhibit enhanced responses against myeloid leukemia. *Sci Transl Med* 2016;8(357):357ra123 doi 10.1126/scitranslmed.aaf2341.
36. Liu E, Tong Y, Dotti G, Shaim H, Savoldo B, Mukherjee M, et al. Cord blood NK cells engineered to express IL-15 and a CD19-targeted CAR show long-term persistence and potent antitumor activity. *Leukemia* 2018;32(2):520–31 doi 10.1038/leu.2017.226. [PubMed: 28725044]
37. Berger C, Berger M, Hackman RC, Gough M, Elliott C, Jensen MC, et al. Safety and immunologic effects of IL-15 administration in nonhuman primates. *Blood* 2009;114(12):2417–26 doi 10.1182/blood-2008-12-189266. [PubMed: 19605850]
38. Perera PY, Lichy JH, Waldmann TA, Perera LP. The role of interleukin-15 in inflammation and immune responses to infection: implications for its therapeutic use. *Microbes Infect* 2012;14(3):247–61 doi 10.1016/j.micinf.2011.10.006. [PubMed: 22064066]
39. Waldmann TA, Lugli E, Roederer M, Perera LP, Smedley JV, Macallister RP, et al. Safety (toxicity), pharmacokinetics, immunogenicity, and impact on elements of the normal immune system of recombinant human IL-15 in rhesus macaques. *Blood* 2011;117(18):4787–95 doi 10.1182/blood-2010-10-311456. [PubMed: 21385847]
40. Guo Y, Luan L, Rabacal W, Bohannon JK, Fensterheim BA, Hernandez A, et al. IL-15 Superagonist-Mediated Immunotoxicity: Role of NK Cells and IFN-gamma. *J Immunol* 2015;195(5):2353–64 doi 10.4049/jimmunol.1500300. [PubMed: 26216888]

41. Conlon KC, Lugli E, Welles HC, Rosenberg SA, Fojo AT, Morris JC, et al. Redistribution, hyperproliferation, activation of natural killer cells and CD8 T cells, and cytokine production during first-in-human clinical trial of recombinant human interleukin-15 in patients with cancer. *J Clin Oncol* 2015;33(1):74–82 doi 10.1200/JCO.2014.57.3329. [PubMed: 25403209]
42. Conlon KC, Potter EL, Pittaluga S, Lee CR, Miljkovic MD, Fleisher TA, et al. IL15 by Continuous Intravenous Infusion to Adult Patients with Solid Tumors in a Phase I Trial Induced Dramatic NK-Cell Subset Expansion. *Clin Cancer Res* 2019;25(16):4945–54 doi 10.1158/1078-0432.CCR-18-3468. [PubMed: 31142503]
43. Christodoulou I, Ho WJ, Marple A, Ravich JW, Tam A, Rahnama R, et al. Engineering CAR-NK cells to secrete IL-15 sustains their anti-AML functionality but is associated with systemic toxicities. *J Immunother Cancer* 2021;9(12) doi 10.1136/jitc-2021-003894.

Author Manuscript

Author Manuscript

Author Manuscript

Author Manuscript

Synopsis

There is interest in harnessing NK cells to generate allogeneic cell therapies. The authors report IND-enabling studies testing the safety and efficacy of engineered PD-L1⁺ NK cells expressing soluble IL15, and supporting a clinical trial for NSCLC.

Author Manuscript

Author Manuscript

Author Manuscript

Author Manuscript

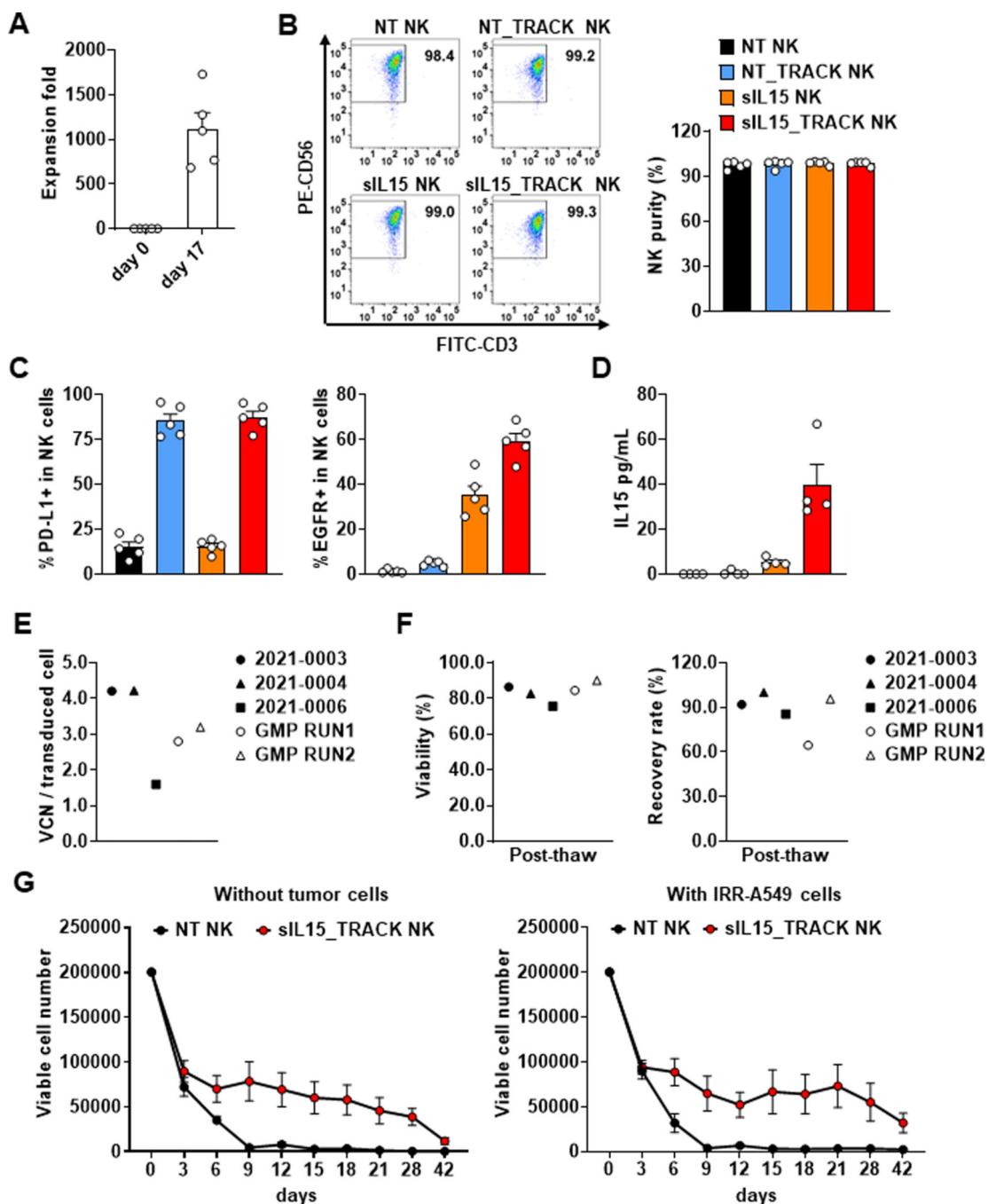


Figure 1: Generation of sIL15_TRACK NK cells.

(A) Primary human NK cells were isolated from umbilical cord blood (UCB) donor units and stored in liquid nitrogen for future use. Post-cryopreserved primary human UCB NK cells were cultured with irradiated K562 feeder cells in the presence of IL2 for 17 days under conditions described in Material and Methods to give either NT NK, NT_TRACK NK, sIL15 NK or sIL15_TRACK NK cells. Summary data on the fold of UCB NK cells on day 0 (baseline) and for sIL15_TRACK NK cells after co-culture for 17 days is shown from 5 different donors. (B) The expression of CD56 and CD3 on NT NK,

NT_TRACK NK, sIL15 NK or sIL15_TRACK NK cells determined via flow cytometry on day 17 before harvesting. Representative flow cytometry plots and the graph summarizing the data from 5 different donors are shown. **(C)** The expression of PD-L1 (PD-L1⁺) and transduction efficiency of soluble IL15 (EGFR⁺) from the same 5 UCB donor units were assessed on day 17 via flow cytometry before harvesting and summarized in graphical format. **(D)** Concentration of human IL15 from 4 different donors was measured in culture medium on day 17 via enzyme-linked immunosorbent assay (ELISA). **(E)** Copy number of the viral vector was determined in sIL15_TRACK NK cells via real-time quantitative reverse transcription (qRT-PCR). Graph summarizing the vector copy number per transduced cell (vector copy number normalized per the rate of transduction) from 5 different donors is shown. **(F)** The viability (%) and recovery rate (%) of sIL15_TRACK NK cells post-cryopreservation is summarized from 5 different donors. **(G)** Enumeration of post-cryopreserved NK cells over the course of 42 days in the absence of any cytokines with or without co-culture with irradiated A549 cells. Summary data are shown from NT NK cells (n = 3) and sIL15_TRACK NK cells (n = 5). NT, Non-transduced; GMP, Good Manufacturing Practice; VCN, vector copy number.

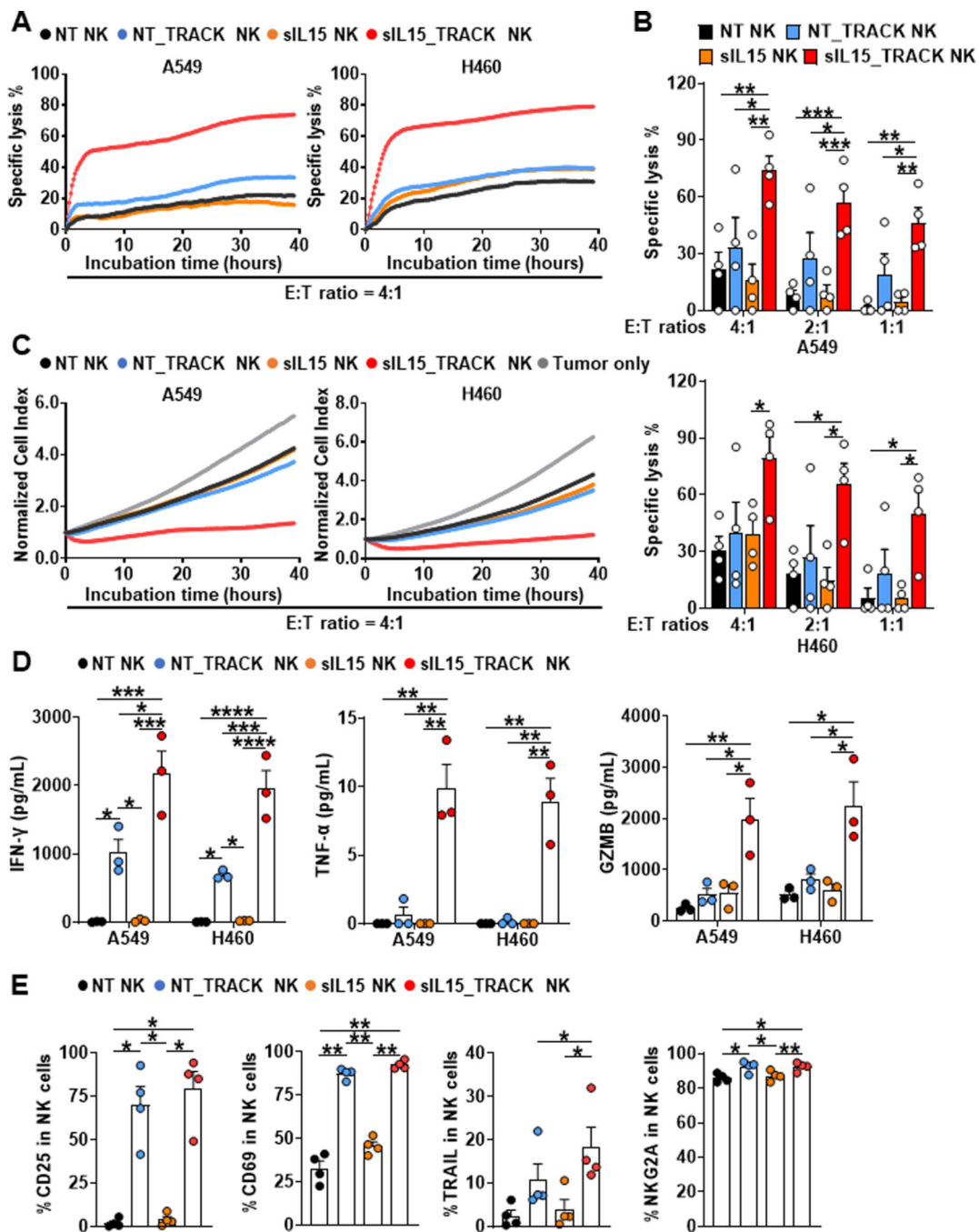


Figure 2: *In vitro* functional activity of sIL15_TRACK NK cells compared to NT NK, NT_TRACK NK, and sIL15 NK.

(A) Representative real-time cell analysis (RTCA) data showing NK cell cytotoxicity against A549 and H460 NSCLC cells at an effector (E)/target (T) ratio of 4:1. (B) Data from the RTCA assay analyzed at three different E/T ratios are summarized for NK cells from 4 different donors. (C) RTCA data showing the growth rate of A549 or H460 NSCLC cells after coculture with NK cells at an E/T ratio of 4:1. (D) Supernatants were harvested after NK cells (1×10^6 /mL) were cocultured with or without A549 and H460 NSCLC cells

respectively at an E/T ratio of 5:1 for 48 hours. Concentrations of IFN- γ , TNF- α and granzyme B (GZMB) were determined via ELISA. Data are summarized from 3 different donors. **(E)** Phenotypic analyses of sIL15_TRACK NK cells and control sIL15 NK cells were determined by flow cytometry. Summary data were analyzed by one-way ANOVA models with repeated measures in **B, D** and **E**. *P* values for multiple-group comparisons were adjusted by the Holm-Sidak method. *, *P* < 0.05; **, *P* < 0.01; ***, *P* < 0.001; ****, *P* < 0.0001. The absence of a *P* value indicates no statistical significance. NK cells used in all experiments were post cryopreservation.

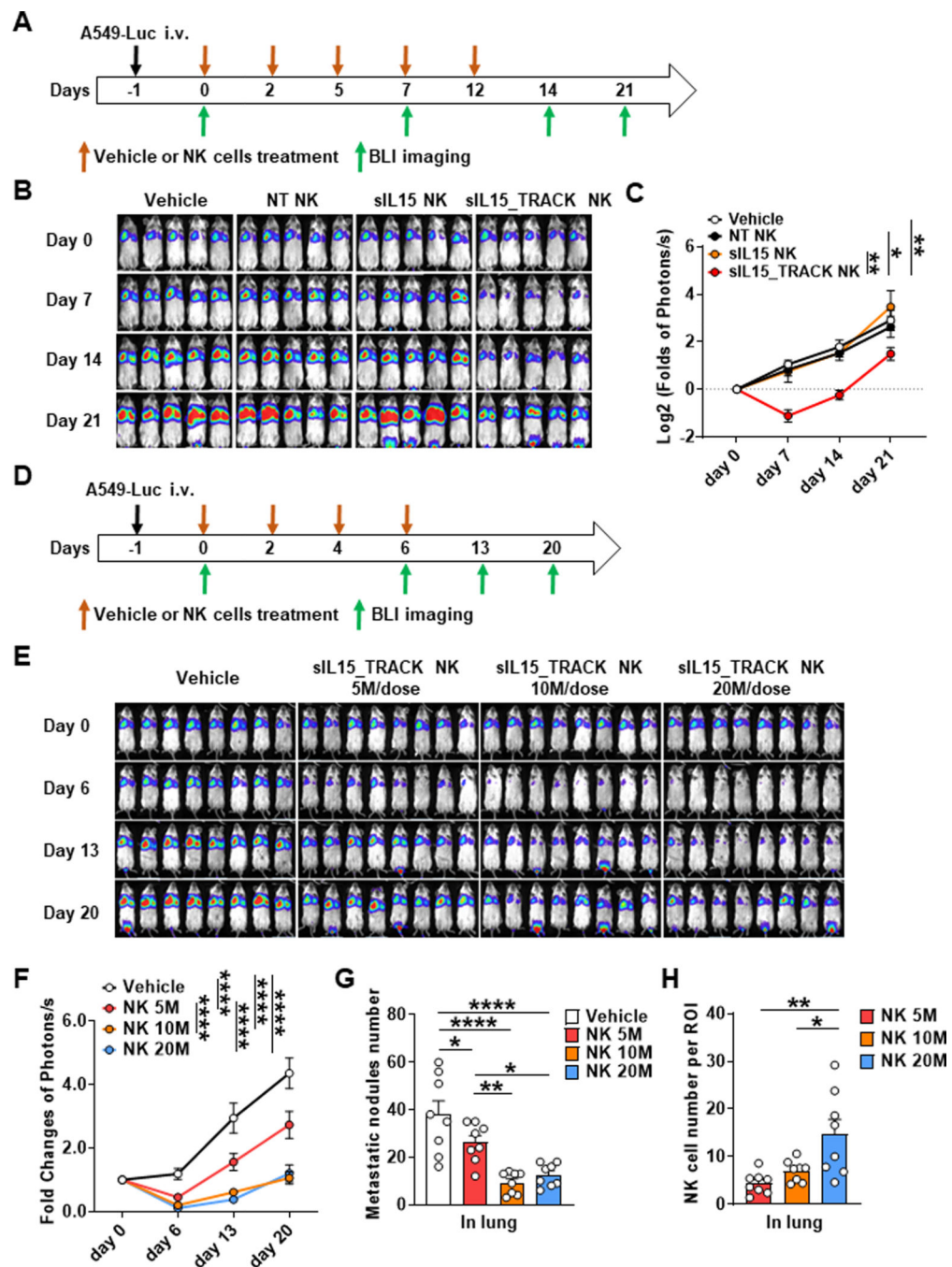


Figure 3: *In vivo* functional activity of sIL15_TRACK NK cells compared to vehicle, NT NK, and sIL15 NK.

(A) Experimental outline: A549_Luc NSCLC cells (0.2×10^6 /mouse) were engrafted into mice by intravenous injection on day -1. Mice were randomly divided into 4 different treatment groups and received treatments including vehicle (PBS), NT NK cells, sIL15 NK cells and sIL15_TRACK NK cells on days 0, 2, 5, 7 and 12. (B) Bioluminescence imaging (BLI) was performed to assess tumor burden on days 0, 7, 14 and 21. (C) Summary BLI data from each time point is shown with statistical analysis of results on day 21.

(D) Experimental outline: A549_Luc NSCLC cells (0.2×10^6 /mouse) were engrafted into mice by intravenous injection on day -1 . Mice were randomly divided into 4 treatment groups including vehicle control (PBS) and three doses of sIL15_TRACK NK cells: 5×10^6 NK cells/dose (5M), 10×10^6 NK cells/dose (10M), and 20×10^6 NK cells/dose (20M) respectively. NK Cells were injected on days 0, 2, 4 and 6. **(E)** Bioluminescence imaging (BLI) was performed to assess tumor burden from **(D)** on days 0, 6, 13, and 20. **(F)** Summary data from each time point is shown with statistical analysis of results on day 20. **(G)** Tumor burden in lungs from mice **(E)** was evaluated. Tumor nodules were defined as being $\geq 50 \mu\text{m}$. Five fields from Regions of Interest (ROIs) per lung were selected, and the number of lung tumor nodules meeting criteria was counted. Summary of tumor burden data are shown (8 mice/group). **(H)** Human NK cell infiltration from **(E)** was evaluated by IHC analysis using the NK cell-specific marker NKp46 in mice lung. Five fields from ROI were selected, and the total number of NK cells was counted. Summary data are shown (8 mice/group). Data were analyzed by two-way ANOVA models with repeated measures in **C** and **F** and one-way ANOVA in **G** and **H**. *P* values for multiple-group comparisons were adjusted by the Holm-Sidak method. *, *P* < 0.05; **, *P* < 0.01; ****, *P* < 0.0001. The absence of a *P* value indicates no statistical significance. Cryopreserved and thawed NK cells were used in this experiment.

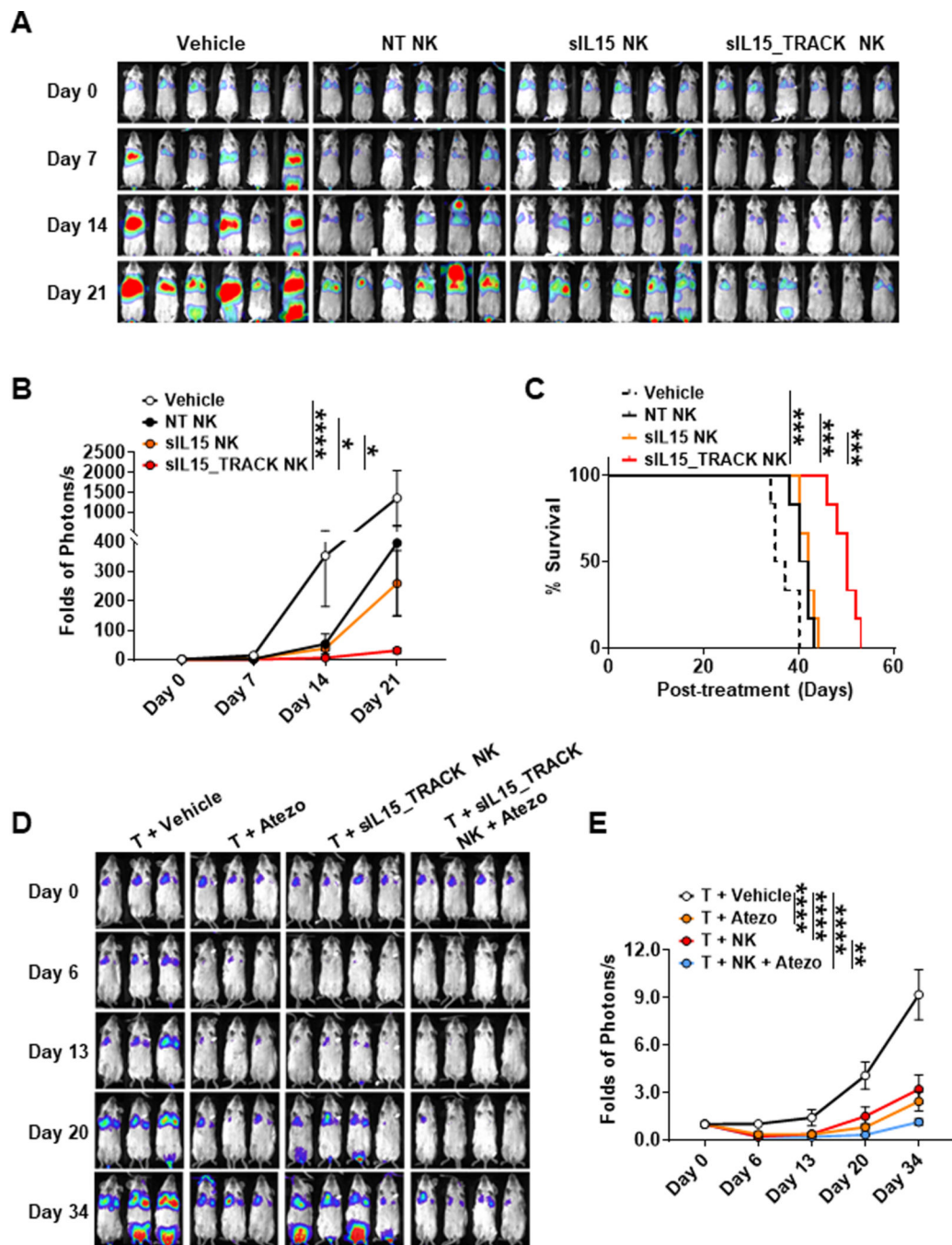


Figure 4: *In vivo* functional activity of sIL15_TRACK NK cells combined with atezolizumab. (A) H460_Luc NSCLC cells (0.15×10^6 /mouse) were engrafted into mice by intravenous injection on day -1 . Mice were randomly divided into 4 treatment groups and received either vehicle control (PBS), NT NK cells, sIL15 NK cells or sIL15_TRACK NK cells (10×10^6 /mouse) on days 0, 2, 5, 7 and 12. Bioluminescence imaging (BLI) was performed to assess tumor burden on days 0, 7, 14 and 21. (B) Summary data from each time point is shown with statistical analysis of results on day 21. (C) Kaplan-Meier plot summarizing survival of mice in each treatment group. $N = 6$ mice/group. (D) A549^{PD-L1}_Luc cells (0.2

$\times 10^6$ /mouse) were engrafted into mice by intravenous injection on day -1 . On day 0, all mice received *ex vivo* expanded 2×10^6 allogenic human T cells. Subsequently, mice were randomly divided into 4 different treatment groups and on days 0, 3, 7 and 10 received either vehicle control (PBS), atezolizumab (0.4 mg/mouse), sIL15_TRACK NK cells (10×10^6 /mouse), or sIL15_TRACK NK cells (10×10^6 /mouse) with atezolizumab (0.4 mg/mouse). Bioluminescence imaging (BLI) was performed to assess tumor burden on days 0, 6, 13, 20 and 34. **(E)** Summary data from each time point is shown with statistical analysis of results on day 34. Data were analyzed by two-way ANOVA models with repeated measures in **B** and **E** and Kaplan-Meier estimates of survival functions plus log-rank test in **C**. *P* values for multiple-group comparisons were adjusted by the Holm-Sidak method. *, *P* < 0.05; **, *P* < 0.01; ***, *P* < 0.001; ****, *P* < 0.0001. The absence of a *P* value indicates no statistical significance. Cryopreserved and thawed NK cells were used in all experiments.

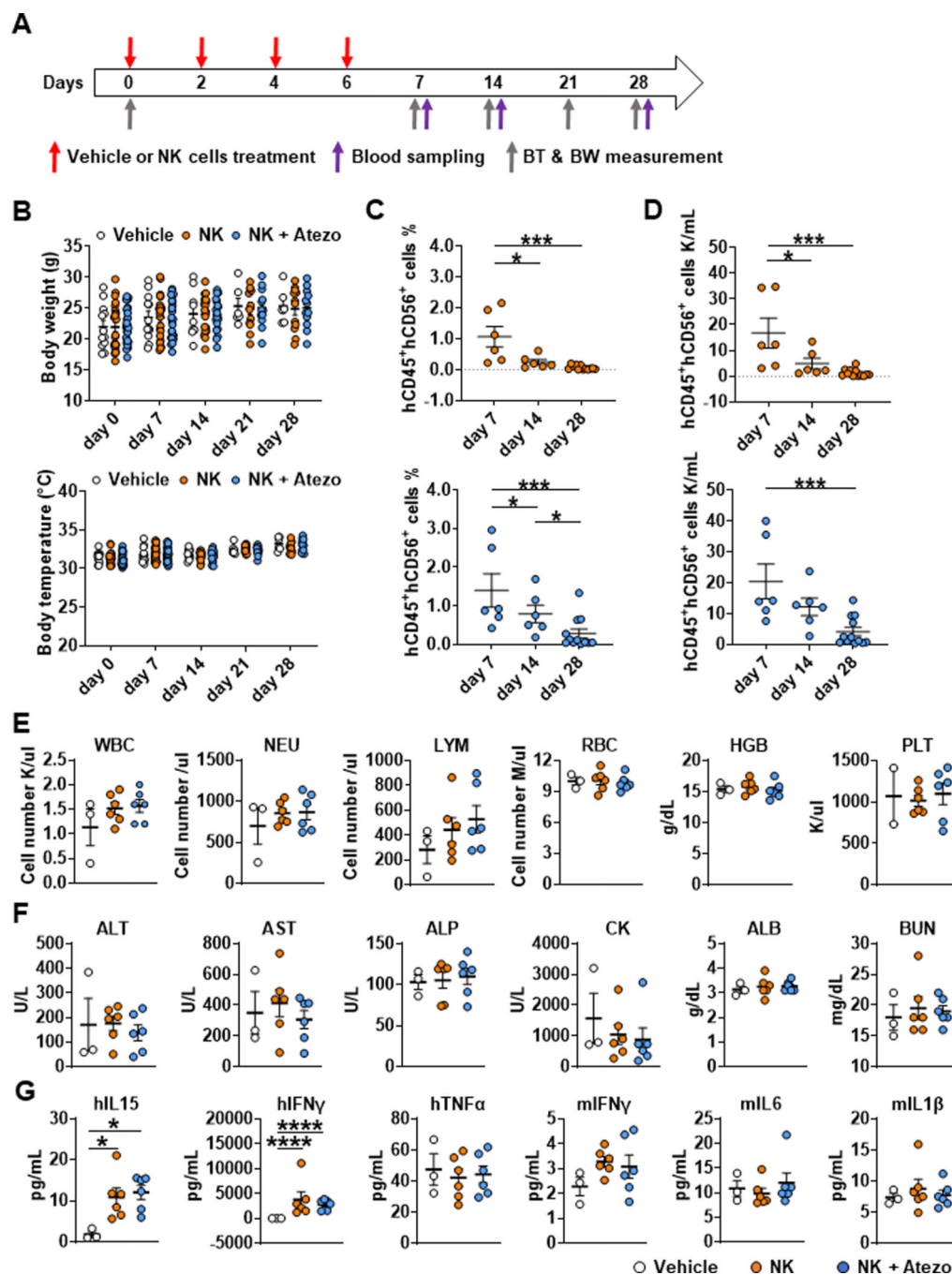


Figure 5: Safety evaluation of sIL15_TRACK NK cells.

(A) Experimental outline: To evaluate the safety of NK cells expressing sIL15 and PD-L1 *in vivo*, NK cells from two different donors (including one GMP product) were injected into mice (10×10^6 /mouse) either with or without atezolizumab (2 mg) on days 0, 2, 4 and 6. There were 12 mice (6 females, 6 male) given vehicle control, 24 mice (6 females and 6 males for each donor) given sIL15_TRACK cells alone, and 24 mice (6 females and 6 males for each donor) given sIL15_TRACK with atezolizumab. During the study, body weight and temperature were measured every 7 days on days 0, 7, 14, 21, and 28.

Three mice per group/per donor were euthanized on days 7 and 14 while the remainder of mice were euthanized on day 28. At each time point CBC, serum chemistry, and NK cell persistence were evaluated. The lung, liver, spleen, and kidneys were also harvested for pathology analysis. **(B)** Body weight (upper panel) and temperature (lower panel) of mice were measured on days 0, 7, 14, 21, and 28. Summary data are shown. **(C)** Blood samples were collected from mice on days 7, 14, and 28. Human NK cells were gated as hCD45⁺hCD56⁺ among live cells. Summary data from animals administered NK cells without (top, red) and with atezolizumab (bottom, blue) are shown separately. **(D)** Absolute numbers of NK cells in 1 mL blood of mice were calculated based on the WBC counts in CBC testing and %hCD45⁺hCD56⁺ evaluated by flow cytometry. Summary data from animals administered NK cells without (top, red) and with atezolizumab (bottom, blue) are shown separately. **(E-G)** Three mice (2 females, 1 male) from each treatment group (vehicle control and from each NK cell donor) were euthanized on day 7. Anti-coagulated blood and sera were collected for CBC **(E)**, chemistry **(F)**, and cytokine profiling assay **(G)**. Dot plots of data are shown. Linear models were applied in **(B)** and one-way ANOVA models in **(C-G)**. *P* values for multiple-group comparisons were adjusted by the Hochberg method. *, *P* < 0.05; ***, *P* < 0.001; ****, *P* < 0.0001. The absence of a *P* value indicates no statistical significance. Cryopreserved NK cells were thawed and used in this experiment. GMP, Good manufacturing practice.